PFC/JA-85-7

LOW-FREQUENCY DENSITY FLUCTUATIONS IN THE ALCATOR C TOKAMAK

R. L. Watterson

Plasma Fusion Center
Massachusetts Institute of Technology
Cambridge, MA 02139

R. E. Slusher, C. M. Surko

AT&T Bell Laboratories
Murray Hill, NJ 07974

February 1985

This work was supported by the U.S. Department of Energy Contract No. DE-AC02-78ET51013. Reproduction, translation, publication, use and disposal, in whole or in part by or for the United States government is permitted.

Low-Frequency Density Fluctuations in the Alcator C Tokamak

R. L. Watterson
Plasma Fusion Center
Massachussetts Institute of Technology
Cambridge, MA 02139

and

R. E. Slusher and *C. M. Surko*
AT&T Bell Laboratories
Murray Hill, NJ 07974

PACS numbers: 52.35.-g, 52.55.Fa

ABSTRACT

CO_2 laser scattering and correlation techniques are used to study low-frequency density fluctuations in plasmas in the Alcator C tokamak. Using crossed-beam correlation techniques, these fluctuations are found to have largest amplitudes near the plasma edge. In discharges with mean plasma densities $\bar{n} \gtrsim 2\times10^{14}$ cm^{-3}, the normalized fluctuation amplitude is $\tilde{n}/n \simeq 0.5$ and peaks at the limiter radius, however at lower plasma densities, $\tilde{n}/n$ peaks in the plasma interior at a normalized minor radius $r/a \simeq 0.75$ (where a is the limiter radius). The radial and poloidal wavevectors of the fluctuations are comparable, with mean wavenumbers $k \sim 20$ cm^{-1}. At any given k, the observed frequency spectrum is broad. For plasma densities $\bar{n} \lesssim 1.5\times10^{14}$ cm^{-3}, the polodial group propagation velocity v_θ of the fluctuations is measured to be approximately 2×10^5 cm/sec in the electron

diamagnetic drift direction, while at plasma densities $\bar{n} \gtrsim 2\times10^{14}$ cm^{-3}, $v_\theta \simeq 9\times10^4$ cm/sec in the ion diamagnetic drift direction. The nature of these fluctuations is also studied in discharges exhibiting boundary-layer instabilities (i.e., "marfes").

Low-Frequency Density Fluctuations in the Alcator C Tokamak

R. L. Watterson
Plasma Fusion Center
Massachussetts Institute of Technology
Cambridge, MA 02139

and

R. E. Slusher and *C. M. Surko*
AT&T Bell Laboratories
Murray Hill, NJ 07974

I. Introduction

Numerous studies have confirmed that tokamak plasmas have density fluctuations with typical wavelengths small compared to the minor radius of the plasma and frequencies of the order of the electron or ion diamagnetic drift frequency.[1,2] The spectra of these fluctuations are found to be relatively broad, both in frequency at fixed wavevector and in wavevector at fixed frequency.[3,4] It is for this reason that they are commonly referred to as a 'turbulence'. The normalized amplitudes of these fluctuations $\tilde{n}/n$ (where n is the local plasma density and $\tilde{n}$ is the density fluctuation amplitude) range from 10^{-2} to 10^{-3} near the center of the plasma to as large as $\tilde{n}/n \lesssim 1$ at the plasma edge.[1-3]

Neither the nature of density fluctuations in tokamak plasmas nor the specific source of free energy which drives these fluctuations is presently understood in detail. It is believed that the turbulence is the manifestation of one or a number of

nonlinear phenomena.[2] However the present state of the theory is such that, while qualitative agreement with various features of the experiments can be achieved; we have yet to reach the state where detailed and self-consistent predictions of the theory describe the experimental measurements.

These turbulent density fluctuations can have several important consequences. The fluctuations can transport particles and energy at a much more rapid rate than that which would be expected on the basis of Coulomb collisions of the plasma particles.[2] For example, there are indications that, at least in small tokamaks with relatively cool plasmas where metal probes can be used, these turbulent density fluctuations can completely account for the particle transport.[5] Whether density fluctuations are responsible for the anomalously large energy transport observed in tokamaks is still an open question.[2]

The large-amplitude density fluctuations observed near the plasma edge (e.g., $0.1 \lesssim \tilde{n}/n < 1$)[1] can also have important consequences. For example, it has now been shown that such a high level of density fluctuations can affect in a profound way the propagation of lower hybrid waves which are launched into the plasma in order to heat and drive currents in tokamak plasmas.[6,7] In addition, it has recently been shown that a very different kind of density fluctuation phenomenon, namely a relatively high-frequency mode with a long wavelength and a sharp frequency spectrum, occurs at the transition to the H-mode (i.e., the high confinement regime) in poloidal-divertor tokamak plasmas.[8] It is, in fact, possible

that this mode is intimately related to the H-mode transition itself.

In this paper, we report studies of the amplitudes, frequency and wavevector spectra, and the propagation velocities of density fluctuations in the Alcator C tokamak using CO_2 laser scattering[9] and correlation[10] techniques. In tokamak plasmas which operate at lower magnetic fields and densities, other choices of scattering wavelength are available (e.g., microwave and far infrared). However the CO_2 laser offers unique advantages for the experiments described here, since refraction effects are negligible even at the highest densities (i.e., $\bar{n} > 1\times10^{15}$ cm^{-3}) achieved in Alcator C, and a large range of wavenumbers (i.e., from 6 to 3000 cm^{-1}) can be studied with only the small angular access to the plasma which is available. The experiments reported here are complimentary to similar studies,[9,10] conducted previously, of low-frequency density fluctuations in the smaller, Alcator A device.

In Alcator C, it is found that the fluctuation amplitude $\tilde{n}/n$ peaks at the limiter radius at mean plasma densities $\bar{n} \gtrsim 1.7\times10^{14}$ cm^{-3} with an amplitude $\tilde{n}/n \sim 0.5$ which extends over a radial extent of the order of one centimeter. (The minor radius of the plasma was typically 16.5 cm.) At lower plasma densities, the fluctuation amplitude is found to peak inside the limiter at $r/a \sim 0.75$, where a somewhat smaller normalized peak amplitude, $\tilde{n}/n \sim 0.1$, is measured. In all cases, both the wavevector and frequency spectra of the fluctuations are broad, with a frequency spread of the order of the mean frequency. Typical mean frequencies

$\bar{\omega}$ are of the order of 150 kHz and typical mean wavevectors $\bar{k}$ are of the order of 20 cm^{-1}.

The net group-propagation velocity of these fluctuations (including plasma rotation) was measured using a delayed-time, crossed-beam correlation technique. In Alcator C, we find that the net velocity of the waves is in the ion diamagnetic drift direction at high plasma densities ($\bar{n} \gtrsim 2.0\times10^{14}$ cm^{-3}) and in the electron diamagnetic drift direction at lower plasma densities.

Finally, in pathological discharges exhibiting a boundary layer instability (in Alcator C termed "marfes"),[11] the spatial distribution of the fluctuations is extremely asymmetric in the vertical direction, typically peaking at the upper limiter. In such discharges, these fluctuations near the upper limiter travel in the electron diamagnetic drift direction even at very high mean plasma densities.

This paper is organized in the following way: In Section II, we desribe briefly the CO_2 laser scattering and correlation techniques with emphasis on changes and improvements in the system relative to the Alcator A experiment. In Section III we present the spectra and spatial distributions of the density fluctuation amplitude for a variety of plasmas in the Alcator C device. Finally, in Section IV, we relate these results to studies of other tokamak plasmas and to current theoretical models of density fluctuations in inhomogenous, magnetized plasmas.

II. Experimental Techniques and Apparatus

The basic techniques used here include small-angle CO_2 laser scattering[9] to measure the wavevector and frequency spectra of the density fluctuations, and correlation of the scattering from crossed CO_2 laser beams[10] which was used to measure the spatial distribution of the fluctuation amplitude $\tilde{n}(\bar{r})$. Since these techniques have been described in detail previously and a similar apparatus was used in the experiments on the Alcator A tokamak,[9,10] we will only briefly describe the apparatus emphasizing the changes and improvements in the system. The one new scattering technique (at least as regards tokamak experiments) reported here is measurement of the propagation velocity of the density fluctuations using a delayed-time, crossed-beam correlation technique. The concept of such an experiment was described previously,[10] and this technique was subsequently used[12] to study the propagation of fluctuations in the ZT-40 reversed-field pinch. In Appendix B, we show that such an experiment measures the group velocity (as opposed to the phase velocity) of the fluctuations.

The Alcator C tokamak has a major radius R_o of 64 cm. The minor radius, a, was varied by use of different limiters. For the experiments reported here, values of a ranged from 7 to 16.5 cm. Optical access to the plasma was achieved along a vertical chord at major radius adjustable from $x = -5$ cm to $x = +5$ cm and from $x = +8$ cm to $x = +17$ cm, where $x \equiv R - R_0$ and R is the major radius of this chord.

The small-angle scattering apparatus is shown in Fig. 1. Scattered light is mixed with a local oscillator beam formed from the same laser and is detected with a Ge:Cu photoconductor. The mean-squared photocurrent i is proportional to the density-density correlation function

$$S(\vec{k}) = \frac{1}{nV} <\tilde{n}^2(\vec{k})> , \qquad (1)$$

where n is the plasma density, V the measurement volume. In Eq. 1, $\tilde{n}(\vec{k})$ is the Fourier component of the density fluctuation at wavevector $\vec{k}$, with magnitude, k, which is related to the scattering angle ϕ by the Bragg condition[9]

$$k = 2k_0 \sin(\phi/2) . \qquad (2)$$

In Eq. (2), k_0 is the wavenumber (i.e., 2π divided by the wavelength) of the incident laser light.

The frequency spectrum of the fluctuations, $S(k,\omega) \propto \tilde{n}^2(k,\omega)$, is obtained from the frequency spectrum of the photocurrent. In this experiment, the laser beam at the plasma had a radius $a_0 = 3$ mm to the 1/e point in electric field. The beam was collimated in order to maximize the wavevector resolution which was $\Delta k \simeq 6\ cm^{-1}$ (HW to 1/e amplitude). The photocurrent was frequency analyzed using a 16-channel filter bank, one channel of which includes all frequencies from 30 to 900 kHz in order to measure the frequency-integrated signal. The other channels were 25 kHz wide FWHM, and covered the range from 25 kHz to 400 kHz. The scattered signals at lower frequencies include MHD effects and the

effects of acoustic vibrations on the optical system, and therefore they were excluded. The filter outputs were rectified and averaged, typically with a 1 msec time constant and were recorded throughout the entire discharge. The scattering angle was adjusted between plasma discharges by a remotely-controlled mirror.

The crossed-beam correlation apparatus is shown in Fig. 2. Initially parallel beams are made to cross at an angle θ of 2.9° by a lens. For this experiment, the beam waists in the plasma are $a_0 = 1.1$ mm in radius at the 1/e electric field point. The waist a_o is chosen to be small compared to the wavelength of the fluctuations, so that the light scattered from the fluctuations will be in the foward direction.[10] The chord-integrated forward scattering from each of the two beams is detected separately. The resulting photocurrents are then correlated to give a measure of the fluctuation amplitude $\tilde{n}(\bar{r})$ near the position of the beam crossing. Specifically, if the separation of the beams Δx at the location of the turbulent fluctuations is less than the correlation length of the fluctuations, then the forward scattering from these fluctuations will contribute to the correlation of the photocurrents. By moving the beam crossing vertically (i.e., in the y direction in Fig. 2), the distribution of the fluctuation amplidue $\tilde{n}(y)$ can be measured.

The spatial resolution of the measurement is determined by the wavevector spread of the fluctuations and the beam diameter. The resolution ρ perpendicular to the laser beam is[9,13]

$$\rho = [8/\bar{k}^2 + 2a_0^2]^{1/2} , \qquad (3)$$

where $\bar{k}$ is the mean wavevector spread in the fluctuations. The resolution along the beams (i.e., in the y direction in Fig. 2) is

$$\Delta y = \rho/\theta >> \rho \, . \tag{4}$$

For the experiments reported here, $\Delta y \simeq \pm$ 4 cm to the 1/e point in $\tilde{n}^2$, and has roughly equal contributions from the wavevector spread $\bar{k}$ and the finite beam size of radius a_0.

We discovered in the course of the Alcator C experiments that the detailed structure of the resolution function depends on the form of the wavevector spectrum S(k). This is described in some detail in Appendix A, where we show that it is important to include as much of the frequency spectrum of the fluctuations in the correlation function as possible in order to minimize the spatial oscillations in this correlation function.

In the experiments reported here, a hard-wired correlator[14] was used to give the normalized, equal-time correlation function of the photocurrents, i_A and i_B from detectors A and B. Specifically, the correlator measured the rms currents I_A and I_B, where

$$I_A(t) = \langle i_A^2(t) \rangle_T^{1/2} \tag{5}$$

and

$$I_B(t) = \langle i_B^2(t) \rangle_T^{1/2} \, , \tag{6}$$

Also measured was the correlation function

$$C_{AB}(y) = \left\langle \frac{i_A(t) i_B(t)}{[i_A^2(t) i_B^2(t)]^{1/2}} \right\rangle_T , \tag{7}$$

where $< >_T$ indicates an average over the time interval $\pm T/2$ about time t, and y is the vertical position of the intersection of the beams in the plasma (see Fig. 2). Typically T was set equal to 1 msec. The signal $C_{AB}(y)$ is proportional to $<\tilde{n}^2(y,t)>_\Omega$, where Ω is the resolution volume described above which is $\Omega \simeq 2\pi\rho^3/\theta$.

The poloidal propagation velocity of the fluctuations (averaged over the vertical resolution given by Eq. 4) was measured by measuring the non-equal-time, crossed-beam correlation function as a function of the vertical position of the beam crossing in the plasma. This technique is described in some detail in Sec. V of Ref. 10. In the present experiment, each of the photocurrents $i_A(t)$ and $i_B(t)$ was digitized for periods of 16 msec at a 1 MHz rate. Then the non-equal-time cross-correlation function $C_{AB}(y,\tau)$ was evaluated numerically, where

$$C_{AB}(y,\tau) = \left\langle \frac{i_A(t+\tau)\, i_B(t)}{[i_A^2(t)\, i_B^2(t)]} \right\rangle_T , \tag{8}$$

and the brackets $< >_T$ have the same meaning as in Eqs. 5-7. As shown in Appendix B, this procedure measures the group velocity (as opposed to the phase velocity) of the fluctuations. Since this measurement is done in the laboratory frame, the measured velocity will include the effects of plasma rotation. Thus the measurement cannot distinguish plasma rotation from propagation in a non-

rotating plasma.

III. Experimental Results

A. Wavevector and Frequency Spectra

Shown in Fig. 3 are chord-averaged frequency spectra measured using small-angle CO_2 laser scattering at fixed wavevector. For these data the laser beam passed through the plasma center. Since the small-angle scattering measures wavevectors oriented nearly perpendicular to the incident laser beam, the data correspond to poloidal wavevectors. As is typical of results from other tokamaks, the spectra are monotonically decreasing as a function of increasing frequency. While broad frequency spectra are almost always observed in tokamaks, some peaking at finite frequency has been observed in microwave scattering experiments using a frequency-shifted local oscillator.[3] In the present experiment, it is likely that both the fact that an unshifted local oscillator is used in the heterodying process (so that positive and negative frequency shifts are combined) and that the data are chord-integrated measurements leads to the masking of any peak at finite frequency which might be present.

Shown in Fig. 4 is the wavevector spectrum S(k) of the fluctuations (including the effects of finite wavevector resolution) integrated over frequency for the same plasma conditions as in Fig. 3. The data show that S(k) is a monotonically decreasing function of k with mean wavevector spread $\bar{k}$ of 22 cm^{-1}. Here, $\bar{k}$ is the 1/e width of the distribution of $\tilde{n}(k)$, which is assumed to have a Gaussian

distribution in k [i.e., see Eq. (A1) of Appendix I].

The frequency spectra in Fig. 3 are well fit by the function

$$S(k,\omega) = A(k)e^{-\omega/\bar{\omega}_k} . \qquad (9)$$

In Fig. 5 is plotted $\bar{\omega}_k$ as a function of k. This curve has roughly a parabolic shape. We cannot accurately measure $\bar{\omega}_k$ at very small k, since at least some contribution to $\bar{\omega}_k$ at $k = 0$ comes from the finite wavevector resolution which is $\Delta k \sim 6\ cm^{-1}$. We have found that the data for $\bar{\omega}_k$ can be represented by the expression

$$\bar{\omega}_k = A + Bk^2 . \qquad (10)$$

For the hydrogen data shown in Figure 5, we find $A = 2.2\times10^4$ Hz and $B = 1615\ cm^2/sec$. The data in Figure 5 include the effects of finite wavevector resolution; deconvolution would have the effect of reducing the value of A (perhaps even to A=0) and increasing the value of B a modest amount ($\lesssim 20\%$). It should be noted that the day-to-day variation in the frequency spectra measured at fixed wavevector is considerable. For example the value of B in Eq. (10) was observed to vary by as much as $\pm 25\%$ for data taken at nominally the same plasma conditions on different run days.

The spectra described in Figures 3-5 were taken with the laser beam passing through the center of the plasma (i.e., near the magnetic axis), thus these data are a measure of the distribution of poloidal wavevectors k_θ.[9] Radial wavevectors can

be studied by moving the laser beam close to the plasma edge. In similar experiments on the ATC and Alcator A tokamaks, it was found that the distributions of wavevectors for $k \sim k_r$ and $k \sim k_\theta$ were very similar,[4,9] but the frequency spectra at fixed wavenumber were narrower for $k \simeq k_r$ than for $k \simeq k_\theta$. In Alcator C, we find that both the k_r and k_θ distributions and the frequency spectra are quite similar. From wavevector spectra measured with $\vec{k}$ oriented parallel to the toroidal magnetic field, we estimate that the parallel component, $k_{||}$, of the fluctuation wavevectors is $k_{||} < 2\ cm^{-1}$ (i.e., $\lambda_{||} \gtrsim 3$ cm). Thus, within the accuracy of our experiments, the edge turbulence in the Alcator C tokamak is a nearly isotropic, two-dimensional turbulence in the plane perpendicular to the magnetic field.

The data shown in Figs. 3-5 were taken over a 50 msec period of the discharge where the current and density are approximately constant. For comparison, in Fig. 6 is shown the time dependence of the chord-integrated signal at a scattering angle corresponding to a wavenumber of $5.7\ cm^{-1}$. Also shown are the mean frequency $\bar{\omega}_k$ at this wavenumber, the chord-integrated plasma density $\bar{n}$, and the plasma current as a function of time. It is interesting to note that, although the chord-integrated fluctuation level varies markedly throughout the discharge as does the plasma density, the mean frequency $\bar{\omega}_k$ and the chord-integrated value of $\tilde{n}/n$ are reasonably constant.

The contribution to S(k) at low k due to low frequency components is

significant, and the filter bank cuts off these components. We can estimate this more accurately using Eq. (9) to extropolate to frequencies below 20 kHz. When this is done, we find a slight change in S(k) from that shown in Fig. 4. It is evidenced primarily by an increase in the lower k components. When this is taken into account, the values of $\bar{k}$ quoted here are decreased by about 10%.

In deuterium plasmas, the mean wavevectors observed are similar to those in hydrogen plasmas. At fixed k, the frequency spectra observed in deuterium are also similar to those observed in hydrogen to with the $\pm 25\%$ variation mentioned above.

The data presented in this paper were taken using a molybedenum limiter. We have also studied plasmas with similar parameters using a carbon limiter. When averaged over wavevector, the frequency spectra from both were found to decrease in a similar manner at high frequency (i.e., $\omega > 2\bar{\omega}$, where $\bar{\omega}$ is the characteristic 1/e roll-off frequency) as

$$\tilde{n}^2(\omega) \sim \omega^{-2.5 \pm 0.1} . \qquad (10)$$

However $\bar{\omega}$ is higher in the case of the carbon limiter by a factor of the order of two. Unfortunately we were unable to do a systematic study to ascertain the origin of this difference (e.g., changes in Z_{eff}, or the temperature or density profiles).

B. The Spatial Distribution of the Density Fluctuations

The spatial distribution of the fluctuation amplitude $\tilde{n}(\bar{r})$ was measured using

the technique of the correlation of crossed CO_2 laser beams. As discussed in Appendix A, care must be taken to include as many of the low frequency (and thus low-wavevector) components as possible in the correlation measurement, so that artificial structure due to oscillations in the spatial correlation function do not confuse the measurement. Shown in Fig. 7 is the spatial distribution of $\tilde{n}^2$ measured by the crossed-beam correlation technique including all frequencies above 7 kHz for a deuterium plasma with mean plasma density $\bar{n} = 2.0 \times 10^{14}$ cm^{-3} at a magnetic field of 8T. The limiter radius was 16.5 cm. In this plasma, the fluctuations peak very near the limiter. The resolution of the measurement is estimated from Eq. (3) to be $\Delta y \simeq \pm 4$ cm; thus the measurement is nearly resolution limited. In Fig. 8 is shown the spatial distribution in a lower density hydrogen plasma with $\bar{n} = 1.2 \times 10^{14}$ cm^{-3} at a magnetic field of 3.8T. In this case, the peak in the fluctuation amplitude is farther inside the limiter, and the spatial extent of the fluctuations is now wider than our resolution (i.e., approximately 12 cm FWHM). Similar results were obtained at these densities at higher magnetic fields (e.g., 7T) which are more typical of the operating parameters of Alcator C. Taking the resolution of the measurement into accout, these data indicate that the layer of fluctuations is approximately 5 cm thick (FWHM). We note that similar results were obtained in the Alcator A tokamak, where the fluctuation amplitude peaked inside the limiter at lower density, but very near the limiter radius at high density. In Alcator C, the characteristic range of densities in which this change occurs was observed to be between $\bar{n} = 1.2 \times 10^{14}$ cm^{-3} and

$\bar{n} = 2.1\times10^{14}$ cm^{-3}; in Alcator A it occured at $\bar{n} \sim 1.0\times10^{14}$ cm^{-3}. We do not have sufficient data from either Alcator A or Alcator C experiments to determine this characteristic value of $\bar{n}$ of the transition to better than $\sim \pm 4\times10^{13}$ cm^{-3}. In this range of $\bar{n}$, where the change in the radial distribution of the fluctuations occurs in Alcator C, the density and temperature profiles are not observed to change appreciably. We note however that the collisionality is changing as $\bar{n}$ and the edge density both increase.

C. Spectra and Spatial Distribution of Fluctuations in "Marfeing" Discharges

As mentioned previously, there is a class of discharges in Alcator C which exhibit, among other effects, variations in the chord-integrated plasma density. These fluctuations have been labeled "marfes", and appears to be due to an (edge) instability at or near the limiter radius which typically occurs at one polodial location.[11] In Alcator C, these fluctuations occur predominantly inside the magnetic axis. Shown in Fig. 9 are crossed-beam correlation results for a "marfeing" discharge with mean plasma density of 3.5×10^{14} cm^{-3} at a magnetic field of 7.4T in hydrogen. When this effect is observed, the fluctuation amplitude typically increases by a factor of ten, and is located at only one edge of the plasma.

Shown in Fig. 10 is a more detailed study of a discharge which exhibits marfes. (This figure, previously published in Ref. 11, was incorrectly labeled; the error is corrected in Fig. 10.) Data are shown both before and after the marfe is evidenced in other diagnostics (such as the interferometer which measures mean plasma

density). As shown in Fig. 10(b), outside the magnetic axis the spatial distribution of the fluctuations measured along the laser beam changes from a state of relative symmetry before the marfe to a very asymmetric distribution after the marfe. However, 4 cm inside the magnetic axis [Fig. 10(a)], this distribution is found to be extremely asymmetric in marfeing discharges even during the current rise phase (i.e., the first 100 msec) of the discharge. This asymmetry of C_{AB} inside the magnetic axis is observed well before the marfe is evident on other diagnostics such as the density interferometer and the H_α emission. The asymmetry of the density fluctuations becomes fully developed early in the discharge (i.e., in the current-ramp phase). During the marfes the edge plasma density also becomes asymmetric,[11] so that it is likely that $\tilde{n}/n$ remains approximately the same while both n and $\tilde{n}$ increase at one edge of the plasma.

Since this distribution of the fluctuations along a vertical chord is observed to be nearly symmetric (top to bottom) in all other types of discharges, the fluctuation measurements appear to be a very sensitive indicator of the plasma conditions which will develop in time into a marfeing plasma. Whether these fluctuations actually cause the marfe is an interesting but, to our knowledge, as yet unanswered question.

D. Amplitude of the Fluctuations

The angularly-resolved scattering experiments do not have significant spatial resolution along the laser beam at the long wavelengths observed here (i.e.,

$\lambda \sim 3$ mm), thus they measure the integral of S(k) along the intersection of the laser beam with the turbulent fluctuations. If we integrate this quantity over wavevector k and assume that the fluctuations are isotropic in the two-dimensional k-space perpendicular to the magnetic field, we obtain $<\tilde{n}^2>_L$, the line integral of the square of the fluctuation amplitude along the laser beam. The procedure by which $<\tilde{n}^2>_L$ is obtained from the scattering and correlation measurements is described in detail in Reference 10.

For high density plasmas, $\bar{n} \gtrsim 2\times10^{14}$ cm^{-3}, the fluctuation amplitude $\tilde{n}$ peaks at the limiter. Since the radial width of the turbulent layer Δr is small (i.e., $\Delta r \simeq 2$ cm) and is not resolved even by the crossed-beam correlation technique, we can only estimate $\tilde{n}/n$. Assuming the edge density is of the order of 1/10 the central density and assuming a path length through the turbulence of 4 cm (i.e., $\Delta r = 2$ cm), we find $\tilde{n}/n \simeq 0.4$ at the limiter radius. At lower density (e.g., $\bar{n} = 1.4\times10^{14}$ cm^{-3}), assuming the turbulent layer thickness Δr is 5 cm, we find a maximum value of $\tilde{n}/n \sim 0.1$. These estimates, which assume a "typical" profile of the plasma density for Alcator C of the form $n(r)-n(a) \simeq n(0)[1-(r/a)^2)]^{0.6}$, are probably accurate to within a factor of two.

E. The Propagation Velocity of the Fluctuations

The propagation velocity of the fluctuations was measured using the delayed-time, crossed-beam correlation technique described above. In Fig. 11 are shown typical data for $C_{AB}(y,\tau)$ as a function of τ for three different locations, y, of the

beam crossing. These data correspond to a deuterium plasma with mean density 2.0×10^{14} cm^{-3}, a magnetic field of 8.0T, and a limiter radius of 16 cm. The time delay at which there is maximum correlation between the forward scattering from the two beams increases linearly with the distance between the beams measured at the vertical location of the peak amplitude of the turbulent layer (which in this case is the limiter radius). Dividing this distance by the time delay of the correlation peak yields a polodial (propagation plus rotation) velocity of 1.4×10^{5} cm/sec in the electron diamagnetic drift direction.

Shown in Fig. 12 are data for the delay time at which $C_{AB}(\tau)$ is maximum as a function of the beam-crossing position y for a plasma at a mean density $\bar{n} = 1.5\times10^{14}$ cm^{-3}. The limiter radius was 13 cm. These data correspond to a group propagation velocity of 3×10^{5} cm/sec in the electron diamagnetic drift direction. For these plasma densities, the fluctuation amplitude $\tilde{n}$ is found to peak inside the plasma at a radius $r/a \simeq 0.7$. At this radius the electron diamagnetic drift velocity is estimated to be approximately 5×10^{4} cm/sec, so it is not possible to account for the observed velocity by the propagation velocity of the linear mode (without plasma rotation).

In Fig. 13 are shown similar data at a higher plasma density of 4.3×10^{14} cm^{-3}. In this case, data correspond to a propagation velocity $v_\theta \simeq 9\times10^{4}$ cm/sec in the ion diamagnetic drift direction. The crossover from the ion to the electron diamagnetic drift direction is found to occur in a range of mean plasma densities

between $\bar{n} = 1.5\times10^{14}$ cm^{-3} and 2×10^{14} cm^{-3}, which is similar to the range of $\bar{n}$ where the fluctuation amplitude switches from peaking at the limiter to peaking in the plasma interior.

The only exception to this behavior, where the fluctuations propagate in the ion diamagnetic drift direction at high plasma densities, is the "marfeing" discharges. In this case, the fluctuations propagate in the electron diamagnetic drift direction at large values of $\bar{n}$. For example, shown in Fig. 14 are data for a "marfeing" discharge using a 16 cm limiter at $\bar{n} = 3.8\times10^{14}$ cm^{-3} in deuterium at a magnetic field of 8T. In this case, the propagation velocity is 8×10^{4} cm/sec in the electron diamagnetic drift direction.

IV. Discussion of the Experimental Results

A. Spatial distribution and spectrum of the density fluctuations

In this paper, we have presented a study of the amplitudes, frequencies and wavevectors of density fluctuations in the Alcator C tokamak over a wide range of operating conditions. Under all circumstances, large-amplitude density fluctuations ($\tilde{n}/n > 0.1$) are observed throughout the duration of the plasma discharge. These fluctuations are observed to have a broad frequency spectrum at fixed wavevector and a broad wavevector spectrum at fixed frequency. In this section we will discuss the significance of these results and try to relate these data to similar observations of fluctuations in other tokamak devices.

The spatial distribution of the fluctuations is observed to change with mean plasma density. Since our measurements provide only modest spatial resolution relative to the plasma size [i.e., ± 4 cm relative to a limiter radius of ~ 16 cm] and since the fluctuations are observed to have a high amplitude and to be strongly localized near the plasma edge, we are only able to study the properties of the fluctuations in the regions where they have the largest amplitude.

The radial position of the maximum fluctuation amplitude $\tilde{n}$ is located in the plasma interior near $r/a \sim 0.7$ at lower plasma density and moves out to the position of the limiter at a line-average plasma density $\bar{n} \simeq 1.7\times10^{14}$ cm^{-3}. This behavior is similar to the results of the Alcator A experiment;[10] however, in that case, the "crossover" density was somewhat lower, namely $\bar{n} \simeq 1.0\times10^{14}$ cm^{-3}. Peaking of $\tilde{n}$ at the plasma edge was also observed on the PLT[17] and PDX[15] tokamaks, the Caltech tokamak,[18] and the PRETEXT[5] and TEXT tokamaks,[19] while indirect evidence for a broader spatial distribution with less peaking at the edge (similar to the low-density Alcator plasmas) has been reported on the ATC tokamak.[4]

The broad wavevector and frequency spectra observed in Alcator C are similar to the results of the Alcator A experiment.[9,10] Mean values of the frequencies and wavevectors observed in the two experiments are compared in Table I. Considering the observed day-to-day variation of these parameters for different discharges in the same device, both devices exhibit fluctuations which have similar scale lengths

and frequencies to within the accuracy of our measurements.

B. Propagation Velocities of the Fluctuations

In Alcator C, measurement of the velocity of the fluctuations in the laboratory frame (including the effects of plasma rotation) reveal that at high plasma densities the fluctuations and/or the plasma at the edge propagate in the ion diamagnetic drift direction. However, at lower densities the fluctuations and/or the plasma further in the interior are found to propagate in the electron diamagnetic drift direction. These measurements appear to be consistent with measurements on the TEXT tokamak,[19] where a similar change in the direction of the propagation velocity is observed (i.e., in ion direction at the plasma edge and in electron direction in the plasma interior). In the TEXT case, it was shown explicitly that the changes in the velocity measured at the plasma edge were not due to changes in the wave propagation velocity but to drift of the plasma caused by variation in the electrostatic potential of the plasma as a function of minor radius. However, in contrast to these experiments (which indicate propagation in the ion diamagnetic drift direction at the plasma edge), in the PDX tokamak at low densities $\bar{n} \sim 3\times10^{13}$ cm^{-3}, the edge fluctuations were observed to propagate in the electron diamagnetic drift direction for both limiter and divertor plasmas.[15]

It is interesting to note that, in Alcator C, the change in radial position of the largest amplitude fluctuations and the change in direction of the measured group velocity of the fluctuations both occur at the same plasma density,

$\bar{n} = 1.7\times10^{14}$ cm^{-3} to within an accuracy of about $\pm 0.2\times10^{14}$ cm^{-3}. One possible explanation of these results is that the plasma rotation velocity changes as a function of radius. As mentioned above, this is precisely the situation observed on TEXT, where the propagation velocity switches sign in a similar manner.[19] Thus when the fluctuations are at the edge they are in a region where the radial electric field points outward yielding a rotation velocity in the ion diamagnetic drift direction, while farther in the plasma interior the waves are observed to propagate in the electron diamagnetic drift direction. If this interpretation of the results presented here is correct, then the underlying question connected with our results is what is the origin of the change in the radial spatial distribution of $\tilde{n}$ which occurs near a mean density $\bar{n} = 1.7\times10^{14}$ cm^{-3}.

It is also worth pointing out that the range of densities $\bar{n}$ (i.e., from about 1.2×10^{14} cm^{-3} to 2×10^{14} cm^{-3}), in which the spatial distribution of the density fluctuations changes from peaking in the plasma interior to peaking at the plasma edge, is in same the range of $\bar{n}$ in which the energy confinement time in Alcator C ceases to increase linearly with $\bar{n}$. Whether these phenomena are related is as yet unclear.

C. Effects on lower-hybrid wave propagation

It has been pointed out that large-amplitude low-frequency fluctuations, such as those observed in Alcators A and C, can have a significant effect on the propagation in the plasma of higher-frequency waves which might be used to heat

and drive currents in tokamaks. These effects have been discussed for waves with frequencies near the electron-cyclotron frequency,[21] and the ion cyclotron frequency.[21] Perhaps the most profound effects occur for lower-hybrid waves where the spectrum of waves launched at the plasma edge by phased wave-guide arrays is confirmed both theoretically and experimentally to change markedly as the waves propagate into the plasma. This case has been considered in detail.[1,6,22] In addition, we now have rather complete data from the Alcator A and C experiments with which to characterize both the lower hybrid waves in the plasma and the low-frequency density fluctuations.

An experimental study of the lower hybrid waves in Alcator C has been described in detail elsewhere.[7] If we assume nominal parameters for that experiment: exciting frequency $f_o = 4.6$ GHz, $\bar{n} = 2\times10^{14}$ cm^{-3} and a plasma density at the limiter of the order of 1×10^{13} cm^{-3}, we find that for a typical lower hybrid wave having a parallel wavelength corresponding to a parallel index of refraction $N_{||}$ of 3, the turbulent edge region represents a distance which is several times the 90° scattering length for the lower hybrid waves. This can result in back-scattering of the wave, severe spreading of the "resonance cone", and significant upshifts in $N_{||}$ as the waves penetrates further into the plasma through the sheared magnetic field.[22] These shifts in $N_{||}$ affect the coupling of the waves to the plasma electrons[1,6,22] and can therefore alter significantly the heating and current-drive efficiency. Thus, in plasmas which have a high level of low-frequency density fluctuations at the plasma edge (e.g., Alcator A and C and PDX), the $N_{||}$

spectrum will probably have to be directly measured in order to determine with certainty the coupling of the waves to the plasma particles. Lacking such a direct measurement, the measured low-frequency density fluctuation spectrum and theory could be used to at least estimate these very significant effects.

V. Concluding Remarks

We have presented a study of turbulent density fluctuations found to be present in plasmas in the Alcator C tokamak. Much of this data can be integrated with the results from other tokamak devices to form a clearer picture of the turbulent fluctuations present in tokamak plasmas. Such data is useful in understanding the implications which this turbulence is likely to have (e.g., for plasma transport, heating and current drive) in future tokamak devices.

The qualitatively new phenomena reported here involve the change in the nature of the density fluctuations in discharges which exhibit the boundary-layer instability termed "marfes". In these discharges we observe that the fluctuations are markedly asymmetric around the periphery of the plasma and that this change precedes the observation of the marfes on other diagnostics. It therefore appears possible that these density fluctuations play a crucial role in the development of the instability.

VI. Acknowledgements

We would like to thank T. R. Gentile and the Alcator physics, operations and

support staff for their extensive help during the course of this experiment. We would also like to acknowledge the technical assistance of J. F. Valley and thank R. D. Bengtson, P. C. Liewer, B. Lipschultz, Ch. P. Ritz, S. Wolfe and S. J. Zweben for useful conversations. During the course of this work, R. E. S. and C. M. S. were visiting scientists at the Plasma Fusion Center at the Massachusetts Institute of Technology. The Alcator project is supported by the United States Department of Energy under contract No. DE-AC02-78ET1013.

APPENDIX A:

Dependence of Crossed-Beam Correlation Measurements on the Form of the Structure Factor S(k)

The principle of the crossed-beam correlation experiment is that the scattered signals from two intersecting laser beams will be correlated when the volumes from which the scattering cones are separated by less than a correlation length of the turbulence. The behavior of this correlation is quite simple when S(k) is a monotonically decreasing function of k. For example, we have previously discussed the situation[10] where

$$S(k) = Ae^{-2(k/\bar{k})^2} . \qquad (A1)$$

In this case, if the beams are separated by a distance Δx at the turbulent layer (see Fig. 1), the correlation between the scattered signals will be[10]

$$C(\Delta x) = e^{-(\bar{k}\Delta x)^2/8} . \qquad (A2)$$

If however S(k) is non-monotonic, additional structure will occur. Let us consider, for example,

$$S(k) = \frac{A(k/k_0)^2}{(1 + (k/k_0)^2)^2} , \qquad (A3)$$

which was chosen to be close to a particular model[10] of the turbulence and for computational convenience. In this case,

$$C(\Delta x) \;\alpha\; e^{-k_0\Delta}(1 - k_0\Delta x) \qquad (A4)$$

Shown in Figure 15 is the instrumental response function calculated from Eq. (A4) for typical experimental parameters of the Alcator C experiment. The minimum in $|C(\Delta x)|$ when the beams are $\Delta x = 1/k_0$ apart at the turbulent layer corresponds to a beam crossing position, $y = 0.5a$. Minima such as this were observed in both experiments on the Alcator C tokamak and the PDX tokamak.[15]

In Fig. 16(a) are shown data from the Alcator C experiment which display a minimum at $y/a = 0.5$ and a peak at $y/a = 0$. While it is possible, in principle, that the density fluctuations have a minimum at $y = 0.5a$, this signature appeared to be independent of discharge conditions and to be the same for plasmas in both the Alcator C and PDX tokamaks. It was then realized that the effect discussed above might be important[16] and could occur as an experimental artifact. The data plotted in Fig. 16(a) were calculated by filtering the time series $i_A(t)$ and $i_B(t)$ by a digital, high-pass filter before $C_{AB}(0)$ was computed to remove frequencies below 25 kHz. Since lower wavenumbers are associated with lower frequencies, this procedure created an apparent S(k) similar to Eq. (A3). The result of correlating the unfiltered data from the same plasma shots is shown in Fig. 16(b). Inclusion of all frequencies above 7 kHz removes the minimum at $y/a = 0.5$. In subsequent measurements, care was taken to include as much of the low frequency spectrum as possible in order to avoid this effect.

APPENDIX B:

The Crossed-Beam Correlation Technique Measures the Group Velocity of the Fluctuations

The delayed-time crossed-beam correlation technique described in Sec. V of Ref. 10 correlates the fluctuation amplitude $\tilde{n}(\mathbf{x})$ at two points $\mathbf{x}$ and $\mathbf{x}'$. By measuring the time delay $\Delta t = t - t'$ at which this correlation function

$$C(\Delta\mathbf{x},\Delta t) = <\tilde{n}(\mathbf{x},t)\tilde{n}(\mathbf{x}',t')> \qquad (A5)$$

is a maximum, one obtains the velocity of the fluctuation $\tilde{n}(\mathbf{x},t)$. In this Appendix, we show that the propagation velocity which one measures with such a procedure is the group velocity, as opposed, for example, to the phase velocity of the fluctuations.

We write the density fluctuation spectrum as

$$\tilde{n}(\mathbf{x},t) = \int n(\vec{k})e^{i(\vec{k}\cdot\vec{x}-\omega_k t+\phi_k)}d^3k \qquad (A6)$$

The fluctuations are assumed to be random in phase, thus

$$<\int e^{i(\phi_k-\phi_{k'})}\, d^3k'> = \delta^3(\vec{k}-\vec{k}') \qquad (A7)$$

Then

$$C(\Delta\mathbf{x},\Delta t) = <\int n(\vec{k})e^{i(\vec{k}\cdot\vec{x}-\omega_k t+\phi_k)}\, n(\vec{k}')e^{-(k'\cdot\vec{x}'-\omega_{k'}t'+\phi_{k'})}\, d^3kd^3k'> \qquad (A8)$$

$$= \int | n^2(\vec{k}) | e^{i(\vec{k}\cdot(\vec{x}-\vec{x}) - \omega_k(t-t)} \, d^3k \qquad \text{(A9)}$$

Assume now that n(k) is peaked about some wavevector $\vec{k}_0$. Then

$$\omega_k \simeq \omega_0 + \left[\frac{\partial \omega}{\partial \vec{k}}\right]_{k=k_0} \cdot (\vec{k} - \vec{k}_c)$$

$$= \omega_0 + \vec{v}_{go} \cdot (\vec{k} - \vec{k}_0) \, , \qquad \text{(A10)}$$

where v_{go} the group velocity

$$\vec{v}_{go} = \left(\frac{\partial \omega}{\partial k}\right)_{k=k_0} . \qquad \text{(A11)}$$

Then

$$C(\Delta\vec{x},\Delta t) = e^{i(k_0 v_{gp} - \omega_0)\Delta t} \int n^2(k) e^{i\vec{k}(\Delta\vec{x} - v_{go}\Delta t)}$$

$$= C(\Delta x - v_{go}\Delta t, \rho) e^{i(k_0 v_{gp} - \omega_0)\Delta t} \qquad \text{(A12)}$$

For a homogeneous turbulence, the maximum in $C(\Delta x,\Delta t) = C(o,\rho) = \bar{n}^2$. Eq. (A12) shows that this maximum in $|C(\Delta x,\Delta t)|$ propagates with the velocity $\Delta x/\Delta t = v_{go}$. If the plasma itself had some net propagation velocity v_o (i.e., a rotation velocity for the experiments described in Sec. IIID), then we would find $\Delta x/\Delta t = v_{go}+v_o$. For $\Delta t = 0$, $C(\Delta x)$ decays in a distance $\Delta x \sim 1/\Delta k$.[10] Inclusion of higher order terms in Eq. (A10) will lead to a more rapid decay in the

correlation in space. Equation (A12) also indicates that, for $\Delta x = 0$, any given correlation decays in a time $\Delta t \sim 1/(v_{go}\Delta k)$.

Note that the derivation above assumes that the fluctuation spectrum is peaked at some wavevector $\bar{k}_0$. For the experimental results presented in this paper, this $\bar{k}_0$ is less than our resolution of 6 cm^{-1} and may correspond to $\bar{k}_0 = 0$.

REFERENCES

1. C. M. Surko and R. E. Slusher, *Science 221*, 817 (1983).

2. P. C. Liewer, Nuclear Fusion (submitted).

3. E. Mazzucato, Phys. Rev. Lett. *48*, 1828 (1982).

4. R. E. Slusher and C. M. Surko, Phys. Rev. Lett. *37*, 1747 (1976).

5. S. J. Levinson, J. M. Beall, E. J. Powers and R. D. Bengtson, Nucl. Fusion *23*, 527 (1984); and S. J. Zweben and R. W. Gould, Nuclear Fusion (to be published).

6. R. E. Slusher, C. M. Surko, J. J. Schuss, R. R. Parker, J. H. Hutchinson, D. Overskei and L. S. Scaturro, Phys. Fl. *25*, 457 (1982).

7. R. L. Watterson et. al., submitted to Phys. Fluids.

8. R. E. Slusher, C. M. Surko, J. F. Valley, T. Crowley, E. Mazzucato, and K. McGuire, Phys. Rev. Lett. *53*, 667 (1984).

9. R. E. Slusher and C. M. Surko, Phys. Fl. *23*, 472 (1980).

10. C. M. Surko and R. E. Slusher, Phys. Fl. *23*, 2438 (1980).

11. B. Lipschultz et. al., Nuclear Fusion *24*, 977 (1984).

12. A. R. Jacobson and P. R. Forman, Appl. Phys. Lett. *41*, 520 (1982); A. R.

Jacobson, M. G. Rusbridge and L. C. Burkhardt, J. Appl. Phys. *55*, 124 (1984); and G. Nalesso and A. R. Jacobson, Appl. Phys. Lett. *45*, 34 (1984).

13. Equation (40) of Reference 9 is, in fact, an exact result. After Ref. 9 was published we discovered an algebraic error in the derivation of Eq. (40), the consequence of which was to change the approximation into an indentity.

14. Lassen Research Corporation, Manton, CA 96059.

15. R. E. Slusher and C. M. Surko, Proceedings of the 1982 International Conference on Plasma Physics (Published by Chalmers Institute of Technology, 1982), Paper 10a:2; K. McGuire et. al., Phys. Rev. Letters *50*, 891 (1983) and *51*, 1925 (1983) (E); and R. Budny, J. Nuclear Mat. *121*, 294 (1984).

16. We are indebted to I. Hutchinson for this suggestion.

17. E. Mazzucato, Phys. Rev. Lett., *48*, 1828 (1982).

18. S. J. Zweben and R. W. Gould, Nuclear Fusion *23*, 1625 (1983).

19. Ch. P. Ritz, R. D. Bengtson, S. J. Levinson and E. J. Powers, Phys. Fluids (December 1984).

20. B. Hui, E. Ott, P. T. Bonoli and P. N. Guzdar, Nuclear Fusion (1981).

21. M. Ono, Phys. Fl. *6*, 990 (1982).

22. P. T. Bonoli and E. Ott, Phys. Fl. *25*, 359 (1982).

Table I

Comparison of Observed Wavevectors and Frequencies from the Alcator A and C Tokamaks

Tokamak	$\bar{n}(10^{14}\ cm^{-3})$	$\bar{k}(cm^{-1})$	$\bar{k}\rho_s$ [a]	$\omega_k/2\pi$ (kHz)
Alcator A	2.6	16	0.13	150[b]
Alcator A	0.25	5	0.3	150[b]
Alcator C	3.5	20	0.13	150[c]
Alcator C	1.5	20	0.4	180[c]

(a) The gyroradius ρ_s is calculated using the electron temperature and the ion mass.
(b) Measured at $k = 10\ cm^{-1}$.
(c) Measured at $k = 20\ cm^{-1}$.

FIGURE CAPTIONS

Fig. 1. Shown schematically is the small-angle scattering apparatus. The laser beam, I, passes vertically through a minor cross-section of the plasma. Light scattered at small angles is directed onto the detector with a movable mirror M_1. The scattered light, S, is detected by its interference (i.e., heterodying) with a local oscillator beam formed from a small portion of the main laser beam. The distance from the plasma to M_1 is much smaller than that from M_1 to the detector, so that the scattered radiation is within the coherent solid angle of the detector.

Fig. 2. The apparatus for the crossed-beam correlation experiment. The shaded area near the plasma edge denotes a case where the density fluctuations are localized in this region. Forward scattering from two laser beams with electric fields E_{01} and E_{02} is detected on two detectors D_1 and D_2 using local oscillator beams $E_{\ell 1}$ and $E_{\ell 2}$. The vertical position of the crossing of the two laser beams is changed by simultaneously moving lenses L_0 and L_S vertically. The detected photocurrents i_1 and i_2 are then correlated to give information about the amplitude of the density fluctuations near the position of the beam crossing.

Fig. 3. Shown are frequency spectra of $\tilde{n}$ (normalized to unity at zero frequency) at fixed wavenumber: (a) 3.2 cm^{-1}, (b) 9.8 cm^{-1}, and (c) 20.3 cm^{-1}. The amplitudes in (b) and (c) have been scaled up by factors of 1.4 and 5.0

respectively. These data are for a hydrogen plasma at a magnetic field of 7.2T, a current of 300 kA, and a chord-averaged density of $3.5\times10^{+14}$ cm^{-3}.

Fig. 4. The density-density correlation function S(k) is shown as a function of wavevector k. Plasma conditions are the same as for Fig. 3. The solid line is a Gaussian fit to the data which yields a 1/e width $\bar{k}$ of 22 cm^{-1}.

Fig. 5. The frequency $\bar{\omega}_k$ as defined in Eq. (9) is shown as a function of wavenumber k. The dashed line is a least-squares fit to the data of the form $\bar{\omega}_k = A+Bk^2$.

Fig. 6. Shown are the time dependence of (a) the scattered signal at $k = 5.7$ cm^{-1}, (b) the mean frequency, (c) the chord-averaged density (modulo 0.56×10^{14} cm^{-3}), and (d) the plasma current.

Fig. 7. The equal-time crossed-beam correlation function $C_{AB}(y)$ is shown as a function of y, the vertical position of the beam crossing. $C_{AB}(y)$ is proportional $\bar{n}^2(y)$. The arrows denote the location of the limiter. These data correspond to a deuterium plasma at mean plasma density of 2.0×10^{14} cm^{-3}.

Fig. 8. The correlation function $C_{AB}(y)$ is shown as a function of y for a plasma with mean density 1.2×10^{14} cm^{-3}. The notation is the same as in Fig. 8. Note that, in contrast to the data in Fig. 9, the fluctuations peak inside the limiter radius.

Fig. 9. Shown is $C_{AB}(y)$ as a function of y for a discharge which is undergoing

"marfeing" fluctuations.

Fig. 10. The vertical distribution of the fluctuations, $C_{AB}(y)$ is shown as a function of y, for a marfeing discharge; for (a) the laser beam 4 cm inside the magnetic axis, and (b) 4 cm outside the magnetic axis. Open circles and solid circles denote respectively data before and after the marfe is evidenced on other diagnostics.

Fig. 11. The delayed-time, crossed-beam correlation function $C_{AB}(y,\tau)$ is shown as a function of time delay τ at three different values of beam crossing position: (a) $y = -14$ cm, (b) $y = -18$ cm, and (c) $y = -22$ cm. The limiter is located at $y = \pm 16.5$ cm.

Fig. 12. Shown is the beam-crossing position y at which the correlation function $C_{AB}(y,\tau)$ peaks at the indicated time delay. The crossed beams pass vertically through the center of the plasma. Solid and open circles refer to the signals from the fluctuations at the upper and lower edges of the plasma respectively; the dashed and solid curves are fits to these data. The slopes of the curves, when divided by the beam crossing angle, yields the propagation velocity of the fluctuations. These data are for a deuterium plasma with mean density of 1.5×10^{14} cm^{-3} at 7.7 T using a 13 cm limiter radius. The solid and dashed lines yield a group propagation of velocity of 3×10^{5} cm/sec in the electron diamagnetic drift direction.

Fig. 13. Time-delay data are shown for a deuterium plasma at a mean plasma density of 4.3×10^{14} cm^{-3} at 11 T using a 16 cm radius limiter. Notation for the symbols and lines is the same as in Fig. 12. The solid and dashed lines indicate a group propagation velocity of 9×10^{4} cm/sec in the ion diamagnetic drift direction.

Fig. 14. Time-delay data for a "marfeing" discharge with mean plasma density 3.8×10^{14} cm^{-3}. The dashed line corresponds to a group propagation velocity of 8×10^{4} cm/sec in the electron diamagnetic drift direction.

Fig. 15. The correlation function $C(\Delta x)$ given by Eq. (A9) is plotted as a function of Δx.

Fig. 16. The correlation function $C_{AB}(y)$ is plotted as a function of y for the two cases: (a) frequencies below 25 kHz were excluded from the correlation function, and (b) only frequencies below 7 kHz were excluded.

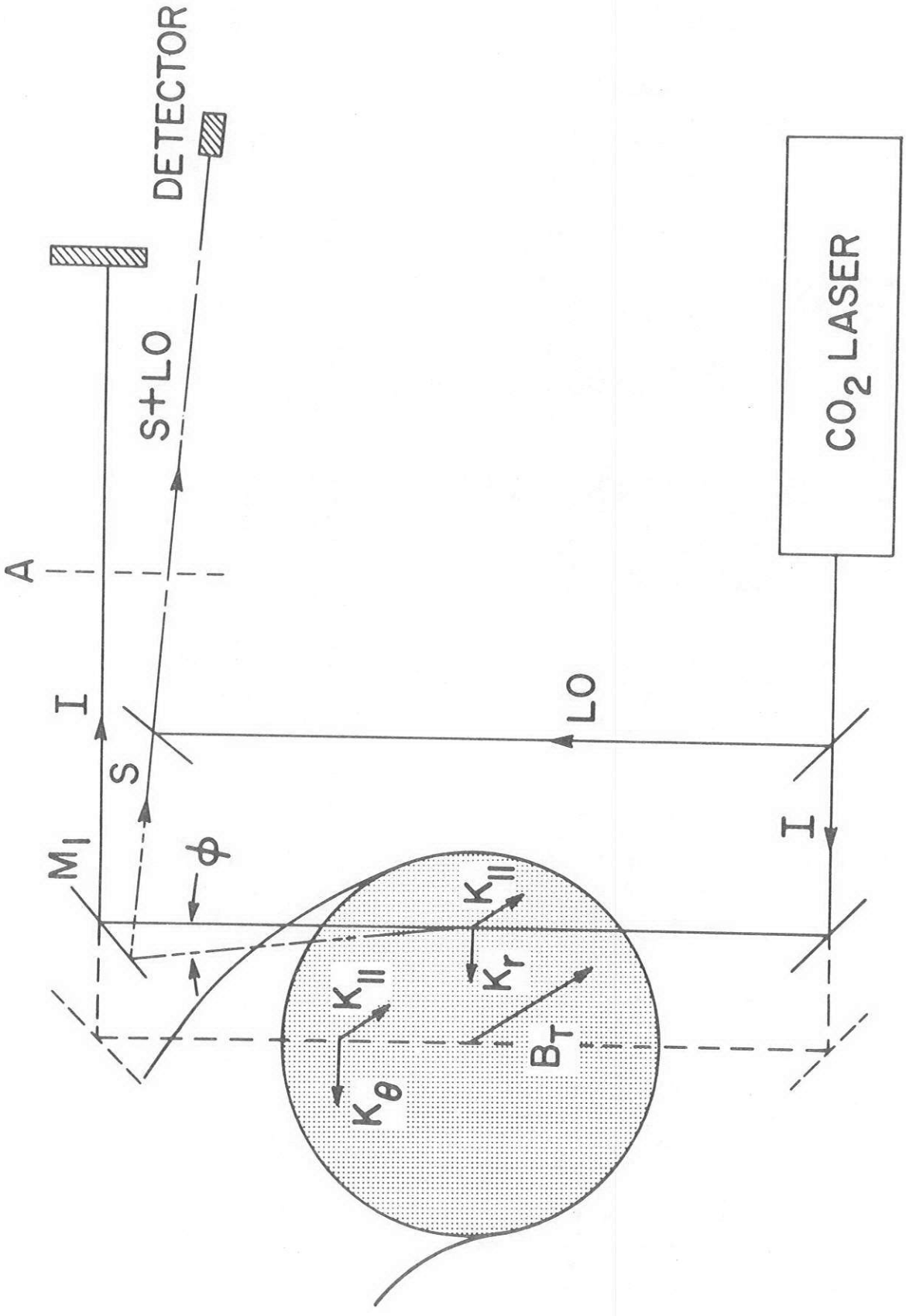

FIGURE 1

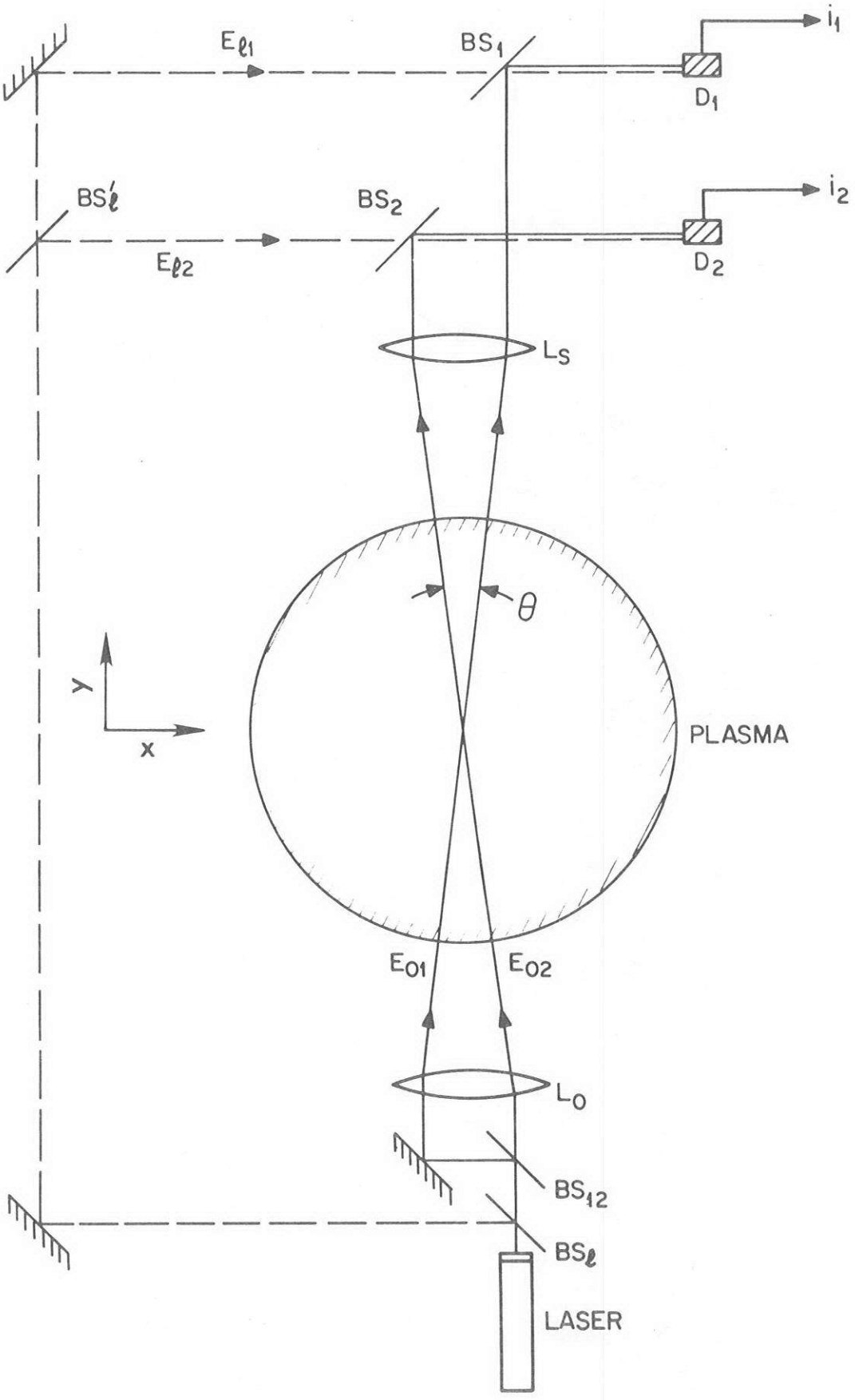
$E_{\ell 1}$
BS_1
i_1
D_1
BS'_ℓ
BS_2
i_2
$E_{\ell 2}$
D_2
L_S
θ
y
x
PLASMA
E_{O1}
E_{O2}
L_O
BS_{12}
BS_ℓ
LASER

FIGURE 2

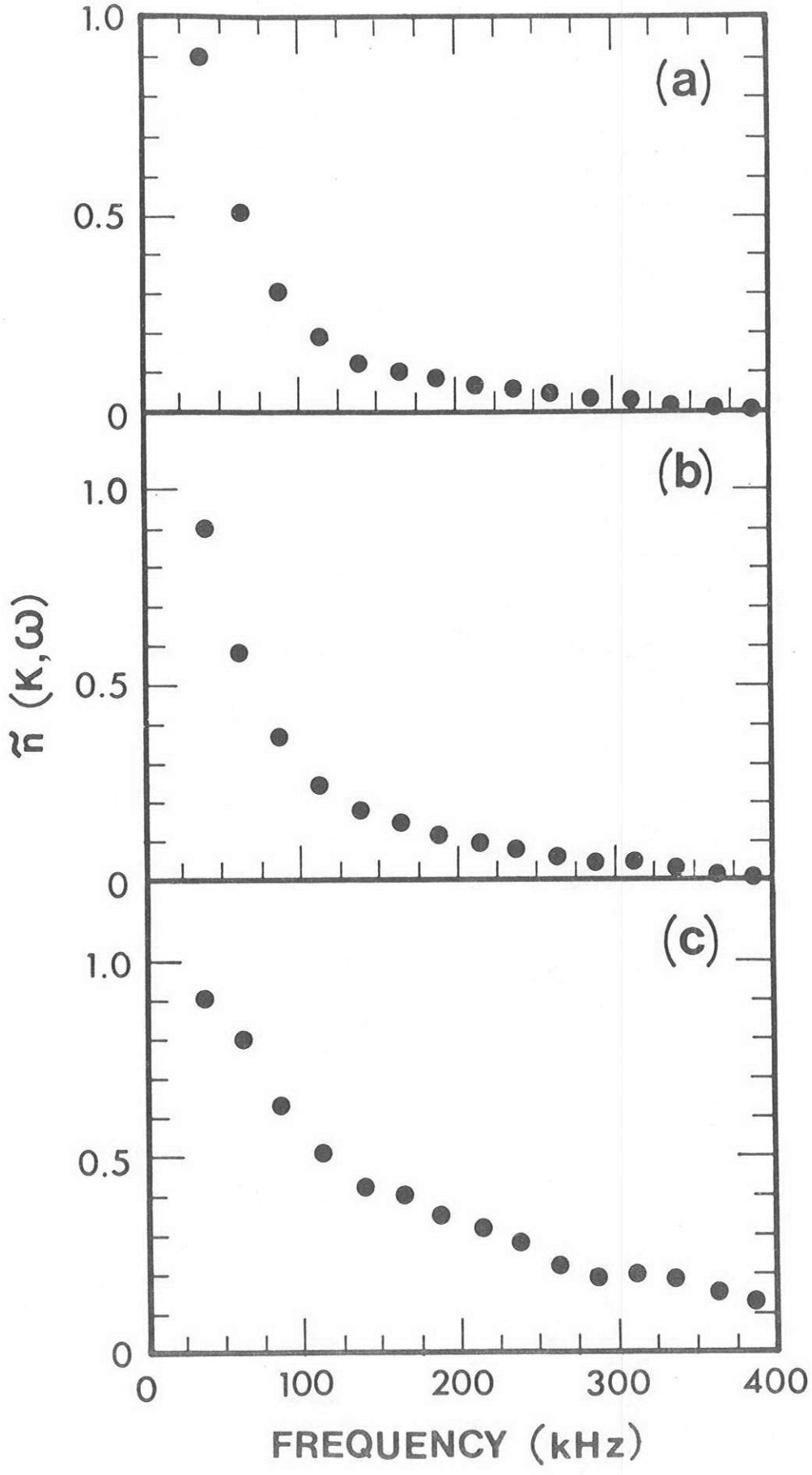

FIGURE 3

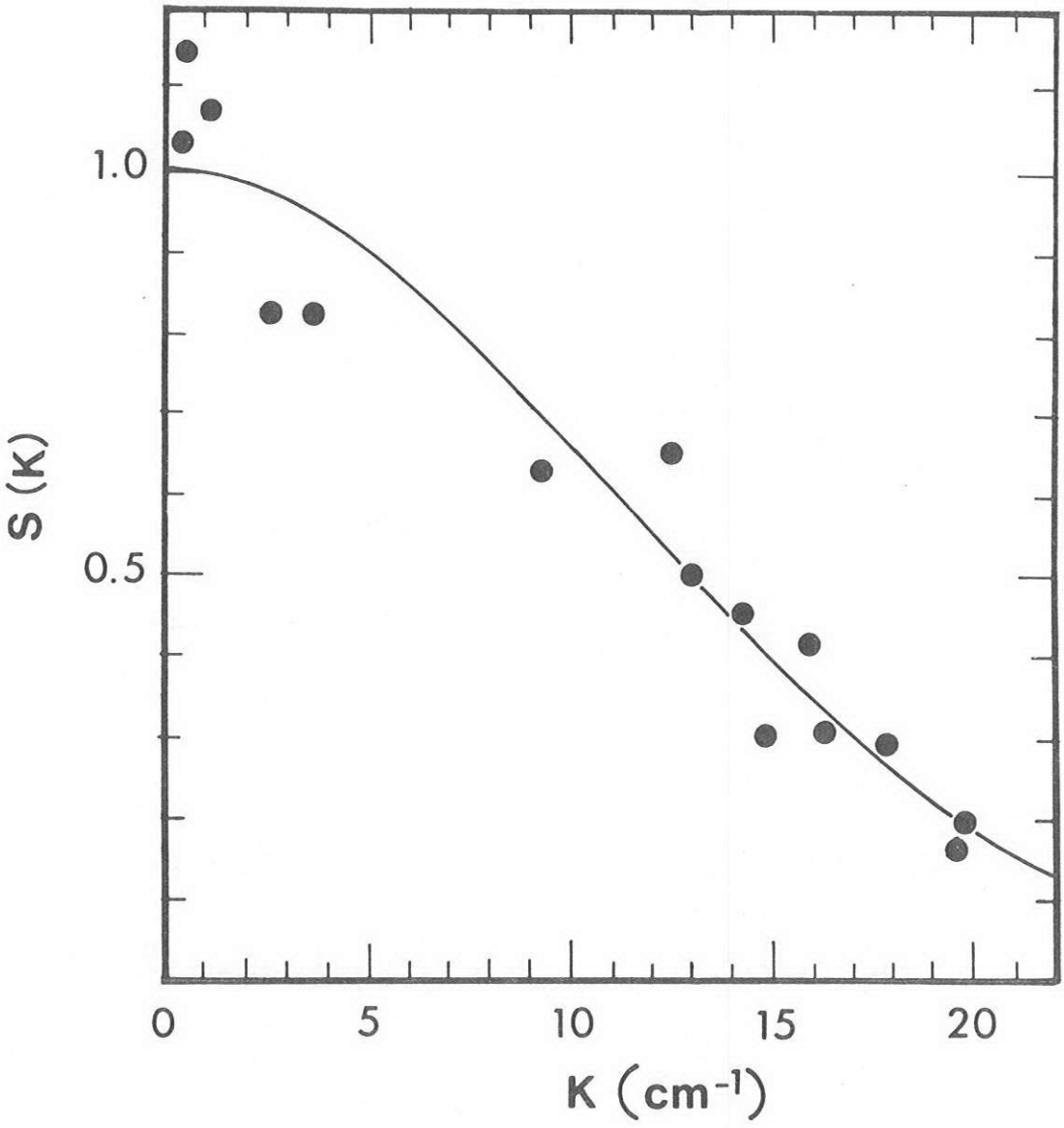

FIGURE 4

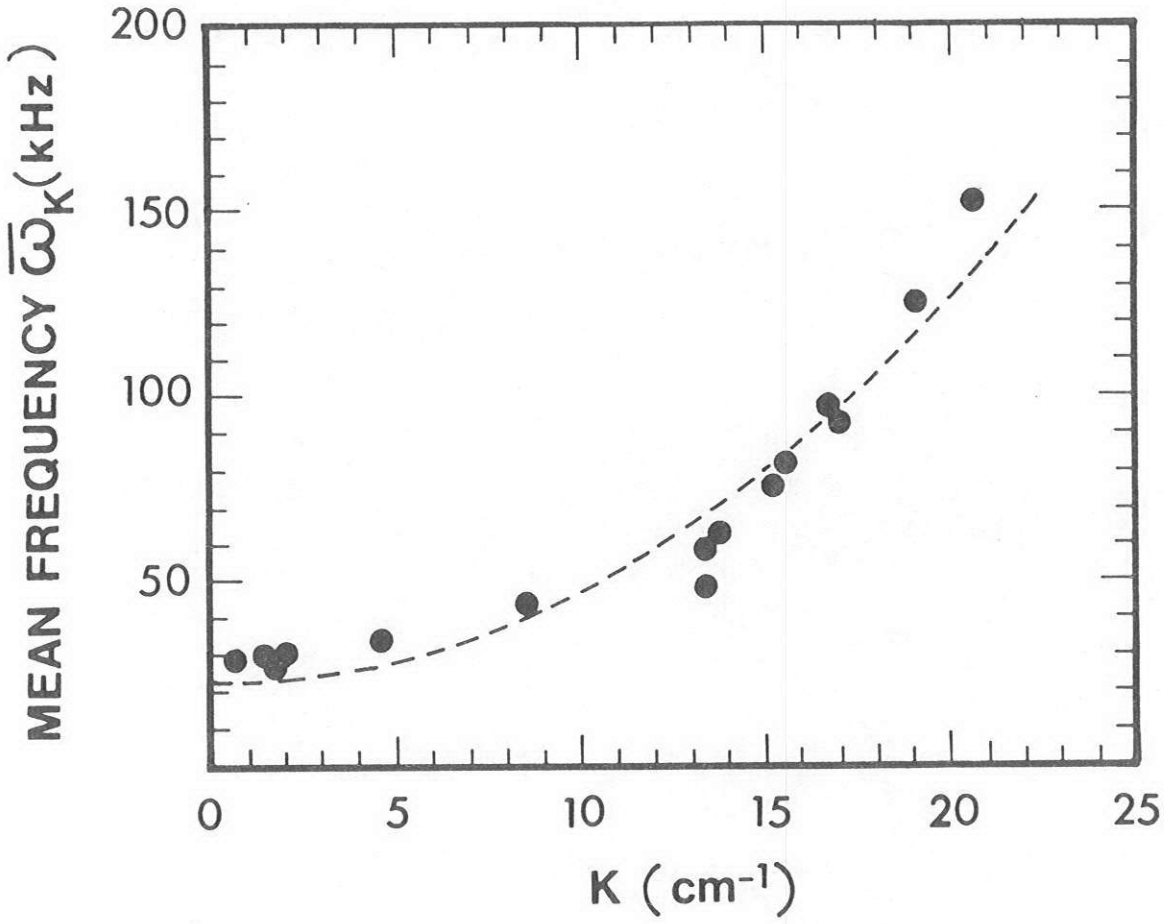
MEAN FREQUENCY $\bar{\omega}_K$(kHz)
200
150
100
50
0
5
10
15
20
25
K (cm^{-1})

FIGURE 5

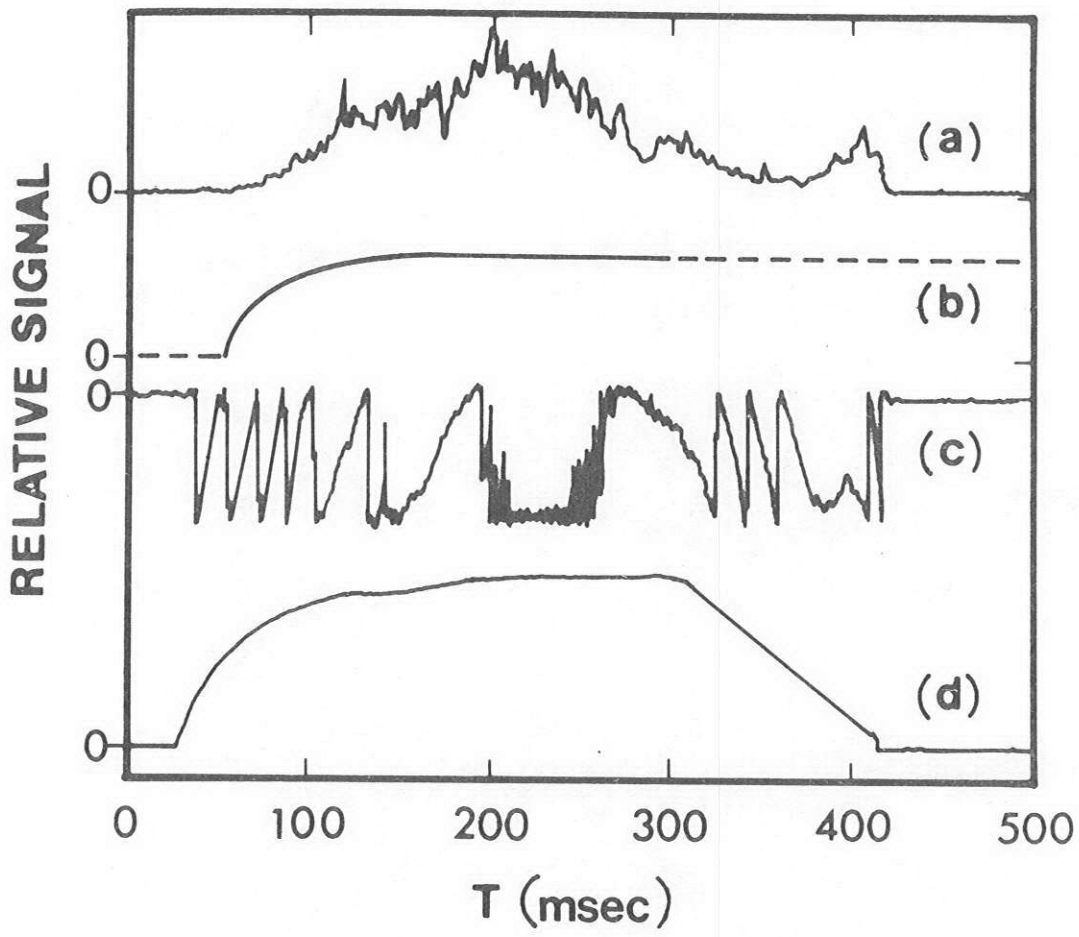

FIGURE 6

8565/17/14

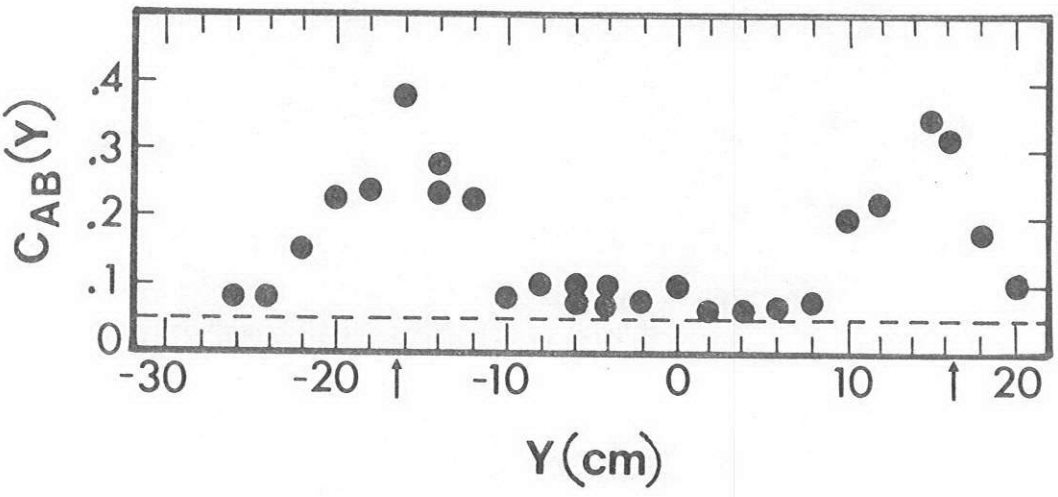

FIGURE 7

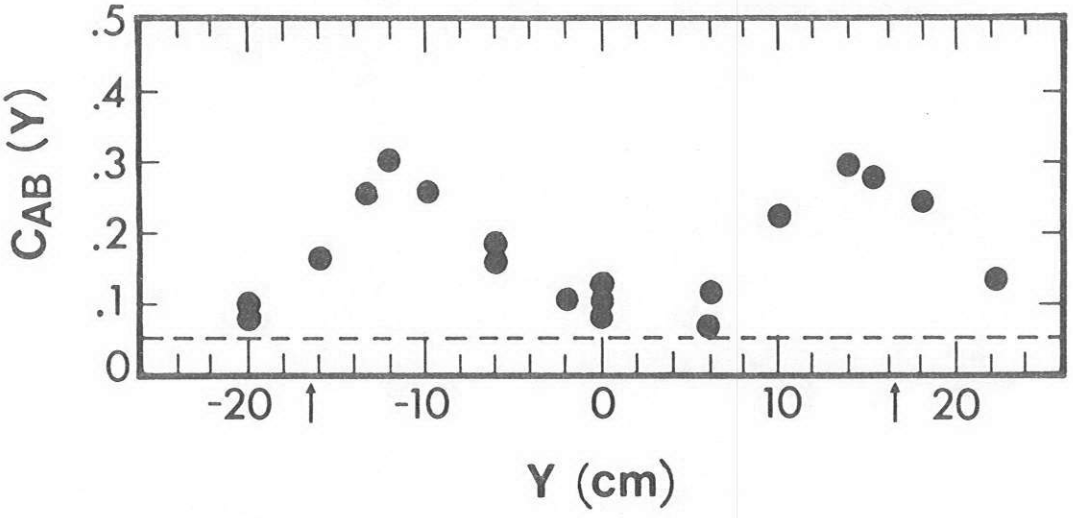

FIGURE 8

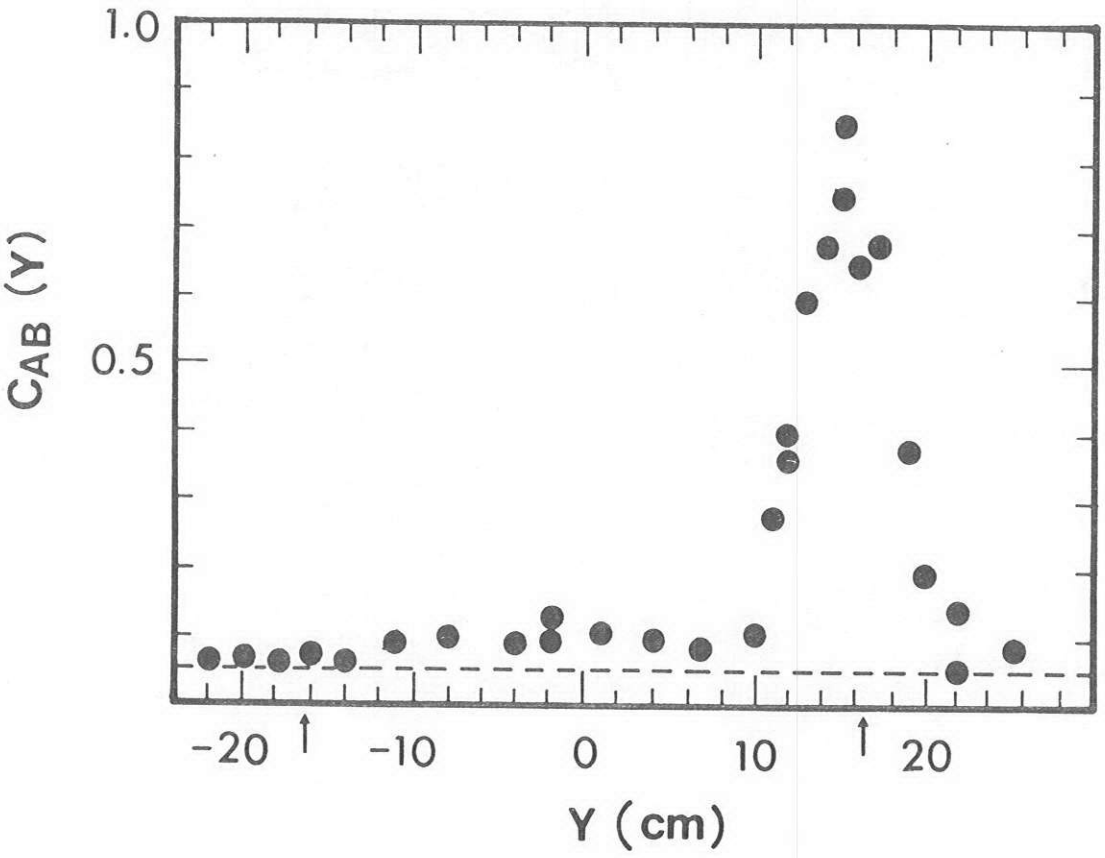

FIGURE 9

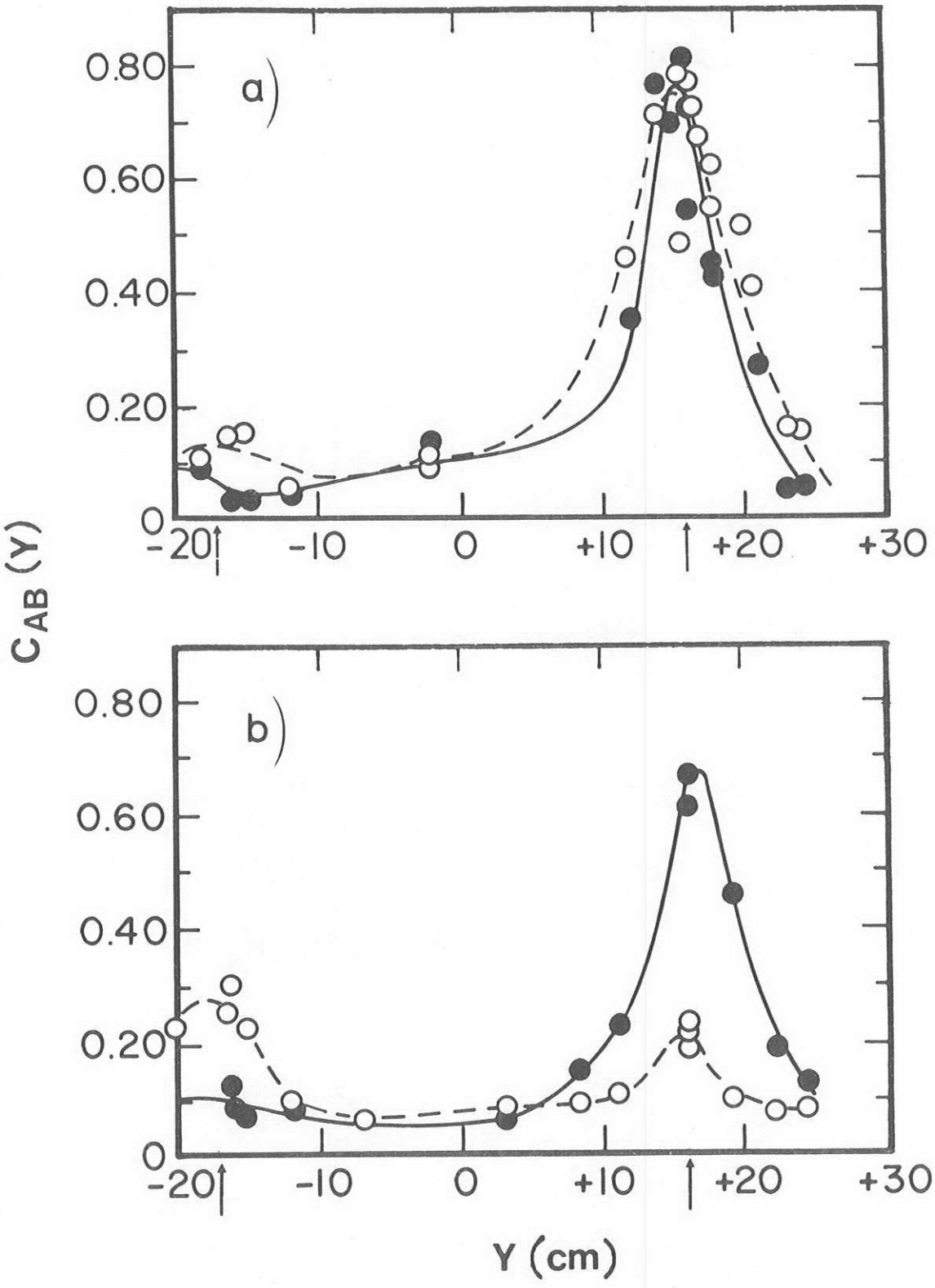

FIGURE 10

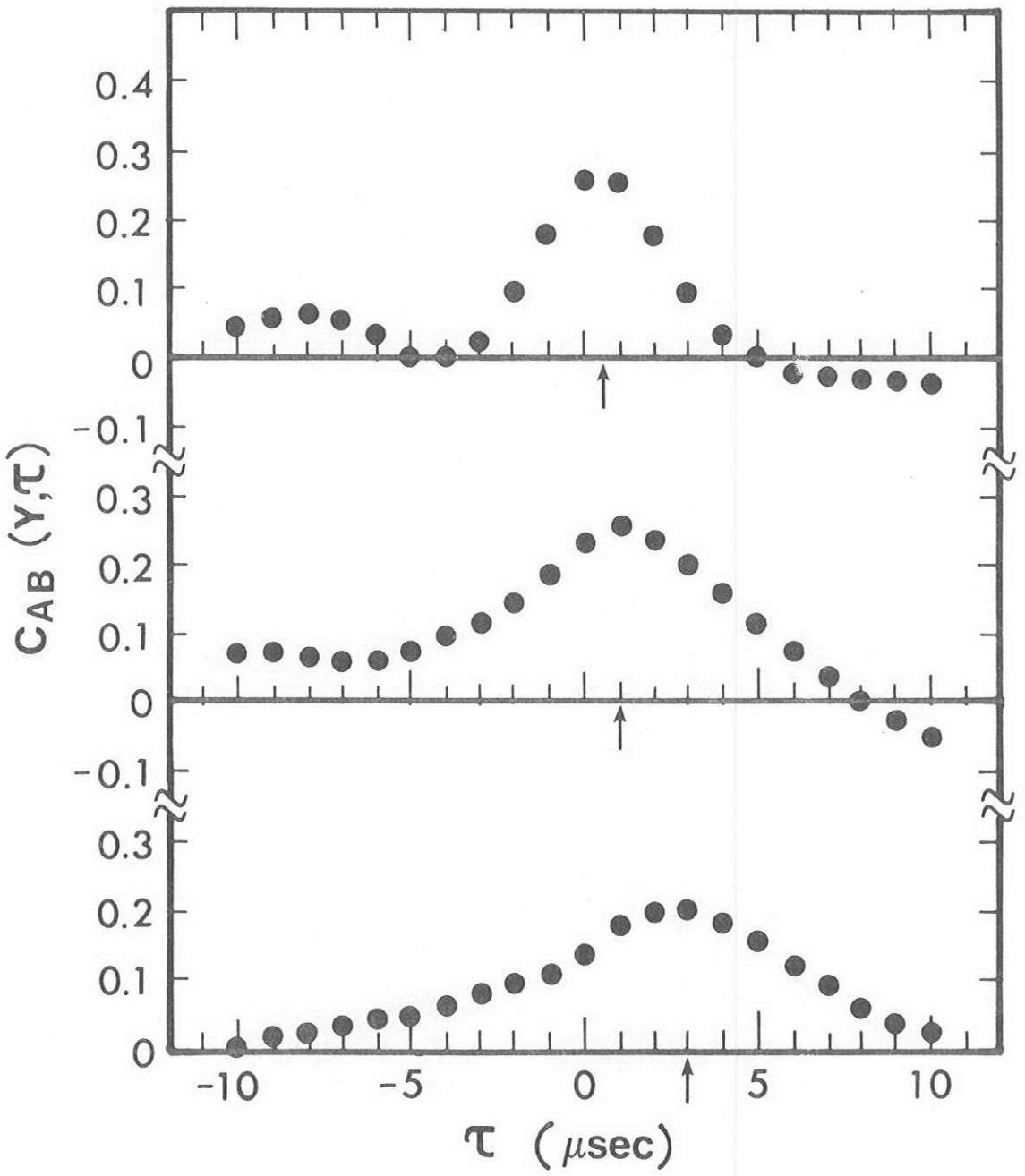

FIGURE 11

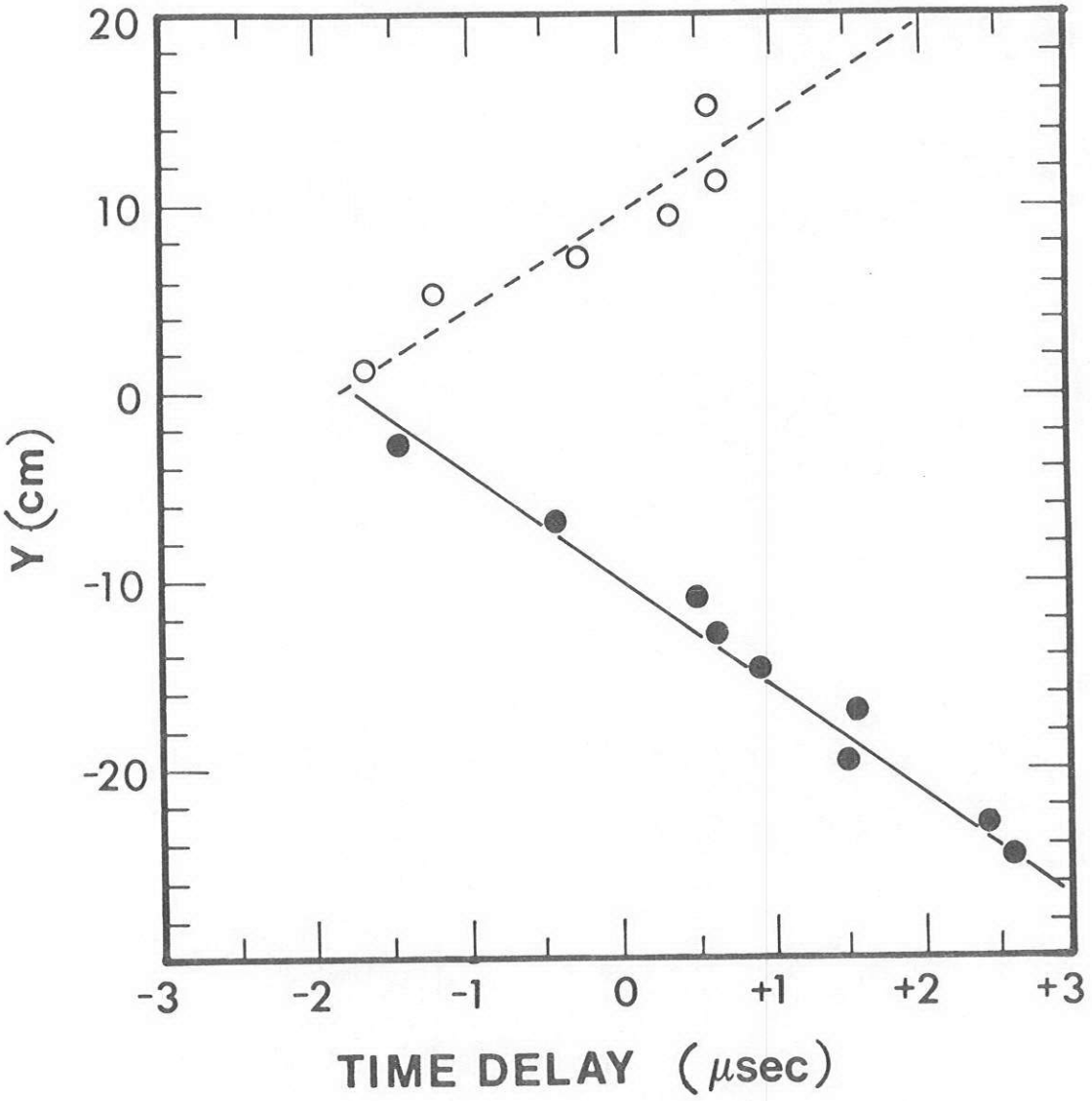

FIGURE 12

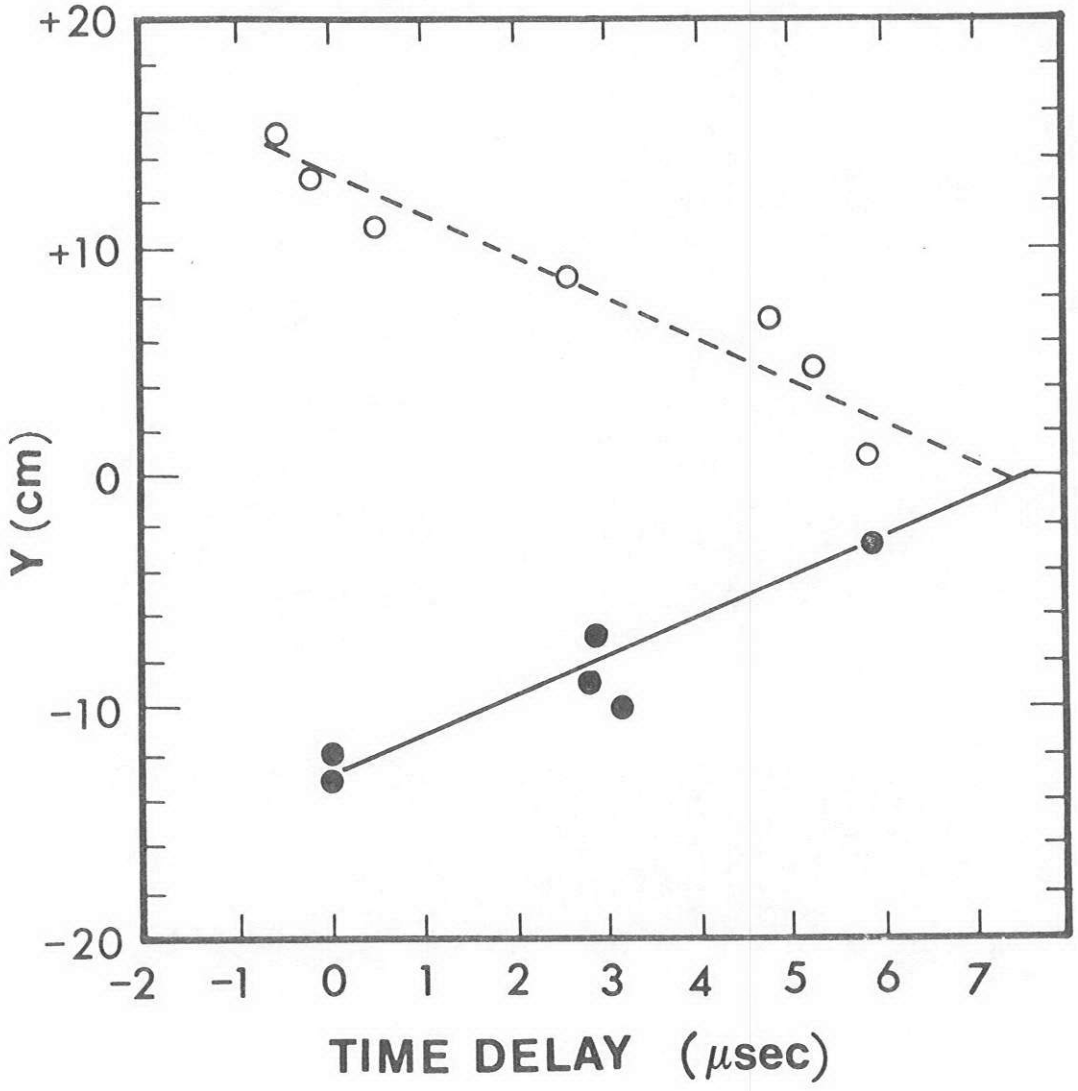

FIGURE 13

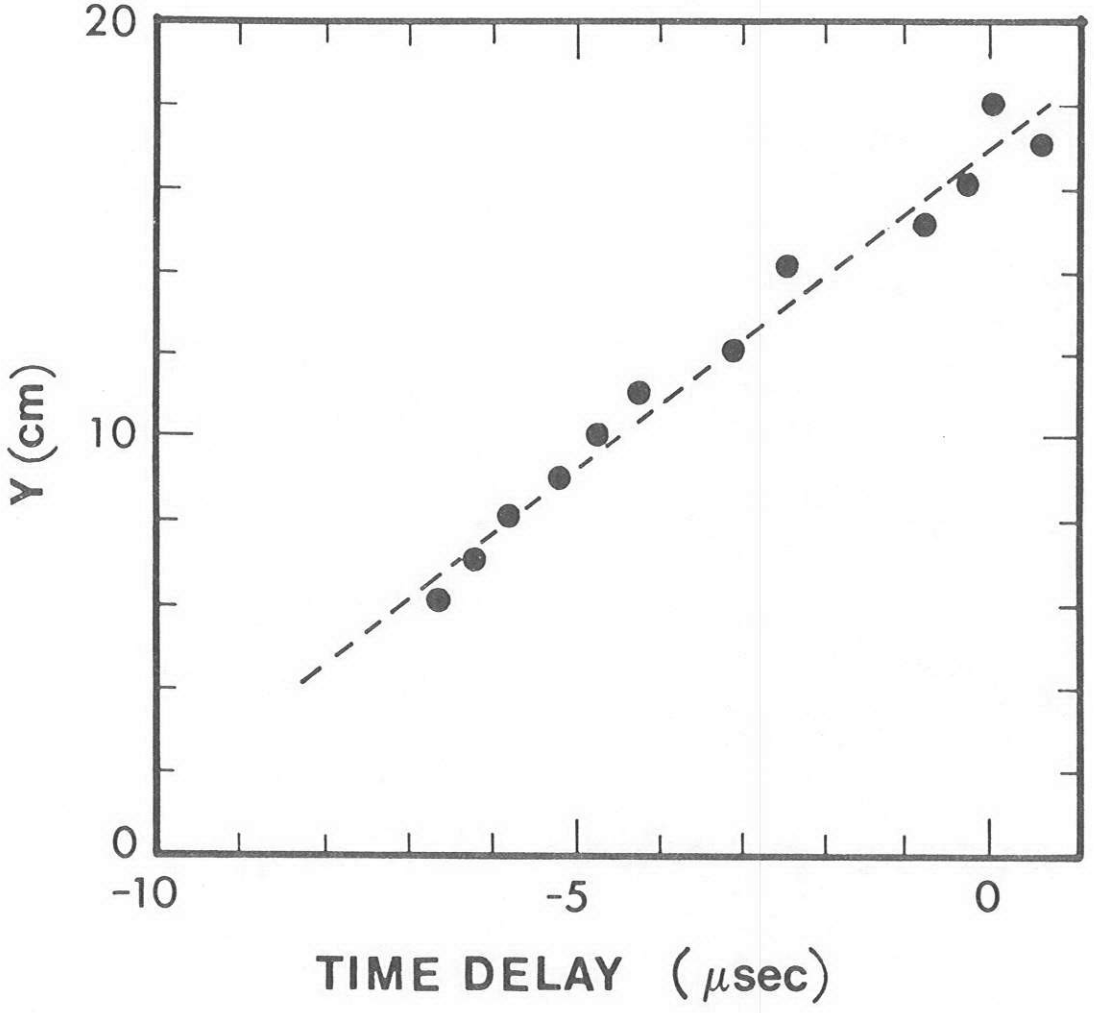

FIGURE 14

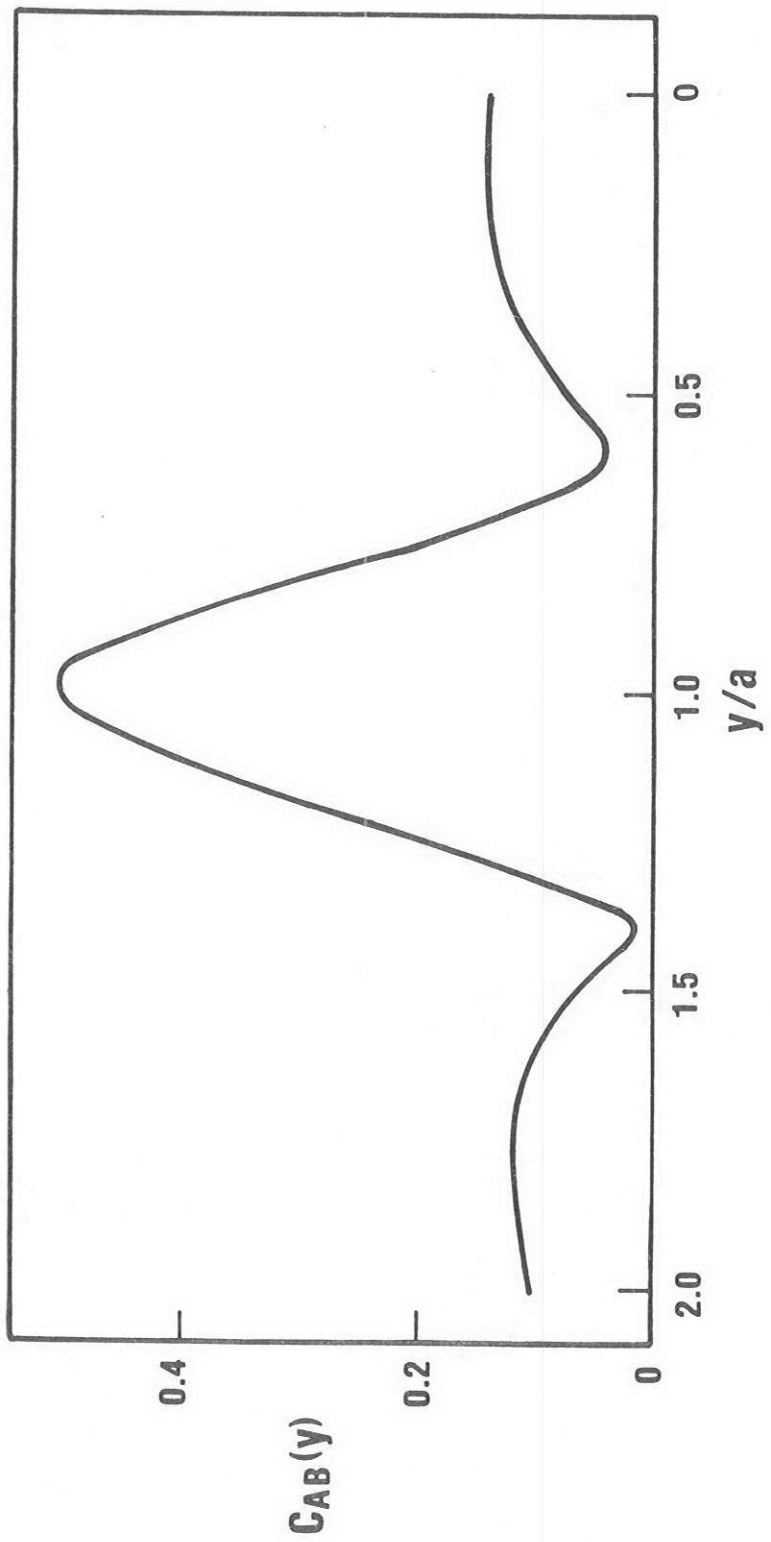

FIGURE 15

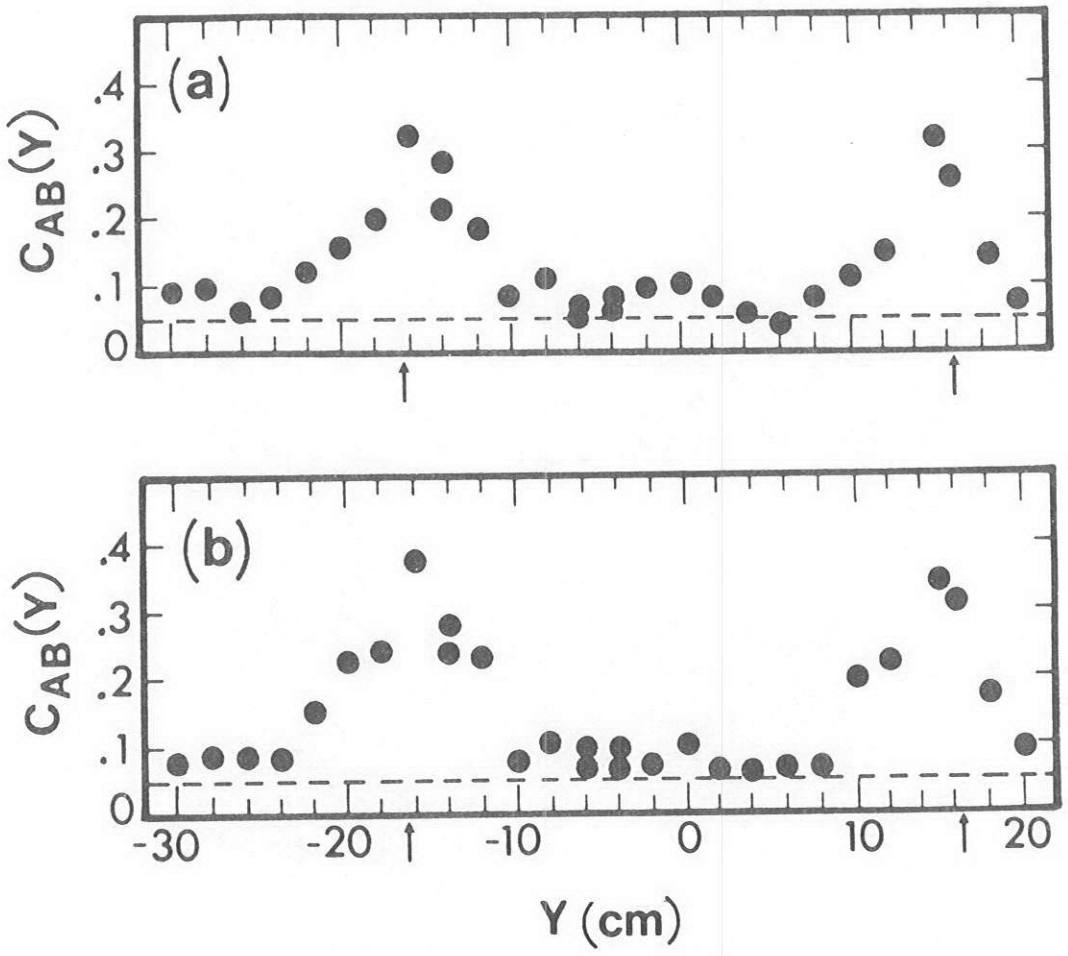

FIGURE 16